

Elastomeric Polymer Multilayer Thin Film with Sustainable Gas Barrier at High Strain

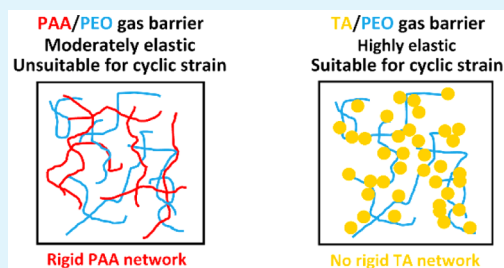
Fangming Xiang,^{†,‡} Tara M. Givens,[†] Sarah M. Ward,[§] and Jaime C. Grunlan^{*,†,§}

[†]Department of Mechanical Engineering and [§]Department of Chemistry, Texas A&M University, College Station, Texas 77843, United States

Supporting Information

ABSTRACT: Most gas barrier thin films suffer from cracking or plastic deformation when stretched, leading to significant loss of barrier. In an effort to make a stretchable gas barrier, which maintains low permeability when exposed to cyclic strain, we prepared layer-by-layer assemblies of tannic acid (TA) and poly(ethylene oxide) (PEO). A 40-bilayer (344 nm-thick) TA/PEO assembly maintained its oxygen transmission rate (6X lower than the 1.6 mm-thick rubber substrate) after being stretched 100%. This submicron coating maintains a barrier 4X lower than the thick rubber substrate even after being strained 20X at 100%. These highly elastomeric assemblies are potentially useful for light-weighting inflatable devices.

KEYWORDS: layer-by-layer assembly, oxygen barrier, cyclic extension, tannic acid, elastic



Layer-by-layer (LbL) assembly is a bottom-up fabrication technique that deposits materials one layer at a time.^{1,2} The thickness of each layer is very small (usually in the nanometer range), so the structure of LbL-deposited thin films can be controlled with nanometer precision.^{3,4} This tremendous level of tailorability results in high performance multilayer assemblies prepared with very little material.⁵ Numerous studies have demonstrated exceptional properties obtained with these multilayer thin films, including gas barrier,^{6,7} fire retardant,^{8,9} and energy generation (and storage).^{10,11} In many cases, multifunctionality is achieved through the use of different interactions, components and structures.^{12–14} For example, an electrically conductive and gas impermeable multilayer coating for electronics packaging was recently developed.¹⁵ An assembly exhibiting both thermal and pH-responsive drug delivery was also demonstrated.¹⁶

A new type of multifunctional LbL assembly, inspired by assemblies exhibiting high mechanical strain^{17,18} and super gas barrier,^{19,20} was recently introduced. This hydrogen-bonded assembly, made with poly(acrylic acid) [PAA] and poly(ethylene oxide) [PEO], could avoid cracking and retain much of its gas barrier up to 100% strain. Strain-induced loss of gas barrier in these PAA/PEO bilayer (BL) assemblies was found to be a result of localized plastic deformation. In an effort to obtain a fully elastomeric gas barrier assembly, PAA was replaced by tannic acid (TA) as the H-bonding donor.²¹ Tannic acid (structure shown in Figure 1a) has a relatively high pK_a and LbL assemblies with TA have been designed to dissociate at or near physiological pH, enabling them to be useful for drug delivery applications.^{22–25} Moreover, its small molecular weight (1701 g/mol) allows TA to have a relatively small molecular size than a true polymer, such as PAA ($M_w = 100\,000$ g/mol).^{21,26} Consequently, it is much easier to eliminate a

network formed by small TA molecules than a network of long PAA chains, because the longer backbone of PAA offers significantly more opportunities for establishing a network through intramolecular H-bonding. The absence of a rigid network allows TA/PEO multilayer assemblies to retain their entire gas barrier even after a single 100% strain. This fully elastomeric gas barrier is a vast improvement over earlier stretchy gas barrier assemblies.^{19,27} These thin films could be suitable for practical applications, involving large and cyclic strains (e.g., inflatable devices).

The assembly of a small molecule (TA) and a soft polymer (PEO) was expected to produce a soft thin film, but the elastic modulus of TA/PEO is highly dependent on deposition pH, as shown in Figure 1a. At $pH \leq 7$, fully protonated tannic acid molecules not only bond with PEO,²¹ but also self-associate through stacking of polyphenolic rings.^{28,29} This self-association establish a continuous and rigid network throughout the assembly, leading to a high modulus (~ 4.7 GPa). Increasing the assembling pH beyond 7 leads to ionization of tannic acid,²¹ which suppresses self-association through inducing negative charges on neighboring TA molecules. In this case, intermolecular H-bonding efficiency is improved and less TA is required to combine with PEO, as suggested by the lower TA content at higher pH (Figure S1b). The combination of reduced self-association, lower concentration, and small molecular size of tannic acid effectively prevents the formation of a rigid network at higher pH. At $pH \geq 8.25$, the modulus of TA/PEO assembly becomes comparable to that of pure PEO (70–100 MPa).³⁰ Similar to previous findings,²¹ the thickness

Received: May 23, 2015

Accepted: July 21, 2015

Published: July 21, 2015

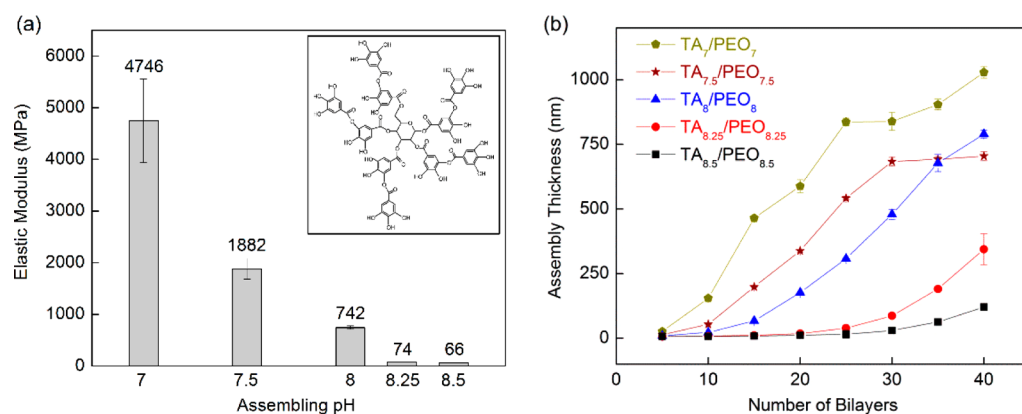


Figure 1. (a) Elastic modulus as a function of deposition pH for 40-bilayer TA/PEO thin films. The inset shows a structural representation of tannic acid from ref 21. (b) Thickness as a function of TA/PEO bilayers deposited at varying pH. Deposition pH is shown as a subscript on TA and PEO.

of TA/PEO decreases with increasing pH, as shown in Figure 1b. Despite showing the lowest modulus, films assembled at pH 8.5 were not evaluated for gas barrier due to very slow and inconsistent growth. Thin films assembled at pH 8.25 (TA_{8.25}/PEO_{8.25}) were used for all of the following experiments due to the best compromise of thickness and modulus.

As shown in Figure 2, a 40-bilayer (344 nm thick) TA/PEO nanocoating reduces the oxygen transmission rate (OTR) of a

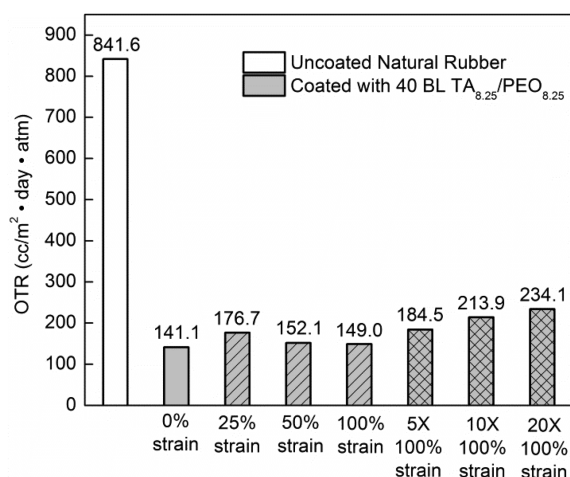


Figure 2. Oxygen transmission rate of 1.58 mm natural rubber sheet, coated with 40-bilayer TA/PEO assembled at pH 8.25, stretched to varying strains and repetitions. Note: Stretching was done under ambient conditions (23 °C, 45% RH), whereas gas barrier testing was conducted at 23 °C, 0% RH.

natural rubber substrate (1.58 mm) by a factor of 6. The permeability of TA/PEO (0.027 Barrer; 1 Barrer = 1×10^{-11} cm³·cm/(cm²·s·mmHg)) is one orders of magnitude lower than that of pure PEO (0.38 Barrer), approaching that of single-crystal PEO (0.0052 Barrer).³¹ Most importantly, TA/PEO does a better job than PAA/PEO in retaining its gas barrier after stretching. As shown in Figure 2, for a single stretch, TA/PEO maintains its entire gas barrier up to 100% strain, while the OTR of PAA/PEO increases by 70%.¹⁹ For films stretched 20 times at 100% strain, the OTR of TA/PEO only rises by 66%, which is significantly lower than the increase for PAA/PEO (140%). This ability of TA/PEO to retain its gas barrier is bolstered by its poststretch surface morphology, which shows no change at any strain level or number of stretches (Figure S2

in the Supporting Information). In contrast, parallel lines are observed on the surface of PAA/PEO as a result of plastic deformation after a single 100% strain.¹⁹

The superior gas barrier retaining capability of TA/PEO is best understood in contrast to the plasticity in PAA/PEO bilayers. Apart from establishing intermolecular H-bonding with PEO, PAA also bonds with itself through intramolecular bonds (Figure 3b).¹⁸ PAA chains are uniformly dispersed

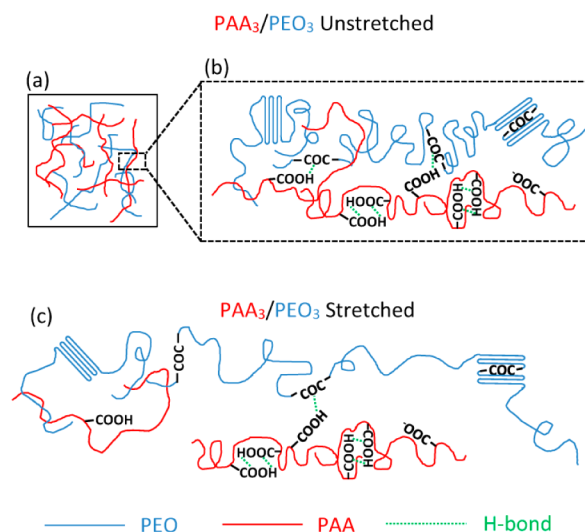


Figure 3. Schematic showing the change in PAA/PEO structure (a, b) before and (c) during stretching.

throughout the PAA/PEO assembly,⁴ so it is quite easy for neighboring polymers to form a continuous network connected by multiple intramolecular H-bonds, as shown in Figure 3a. It should be noted that the parallel aligned chains in Figure 3b,c represent crystallized PEO, which can maintain a partially crystallized structure in a H-bonded assembly.²⁰ Although the efficiency of intramolecular H-bonding can be reduced by greater PAA ionization at higher pH (≥ 2.75), the network cannot be completely destroyed due to the ubiquitous existence, stable concentration, and numerous bonding sites along PAA backbone.^{4,18} When PAA/PEO bilayers are stretched at room temperature (Figure 3c), PEO chains can readily reorient and extend because of high backbone flexibility. In contrast, PAA is very rigid ($T_g \approx 100$ °C).¹⁸ The only way for the PAA/PEO assembly to accommodate extension is by

breaking up the rigid PAA network (Figure 3c), creating plastic deformation. PEO ($-56\text{ }^{\circ}\text{C}$) has a lower glass transition temperature than PAA ($99\text{ }^{\circ}\text{C}$), so it has far more chain flexibility. Because of the big mismatch between PAA and PEO chain segment mobility, many intermolecular H-bonds between PAA and PEO are likely broken during stretching, leading to a further reduction in gas barrier.

Similar to PAA/PEO, the self-association of tannic acid within TA/PEO assemblies becomes less effective at higher pH, but this is where similarity ends. The content of the tannic acid can be reduced by increasing deposition pH (see Figure S1), and the TA molecule is much smaller than PAA. In this case, no rigid network can be formed at higher pH (≥ 8.25) because of less self-association, reduced concentration in the film, and small size of the TA molecules. TA effectively acts a small molecule cross-linker between flexible PEO chains, posing very little restriction to chain segment mobility within the TA/PEO assembly (Figure 4a). The H-bonding between TA and PEO

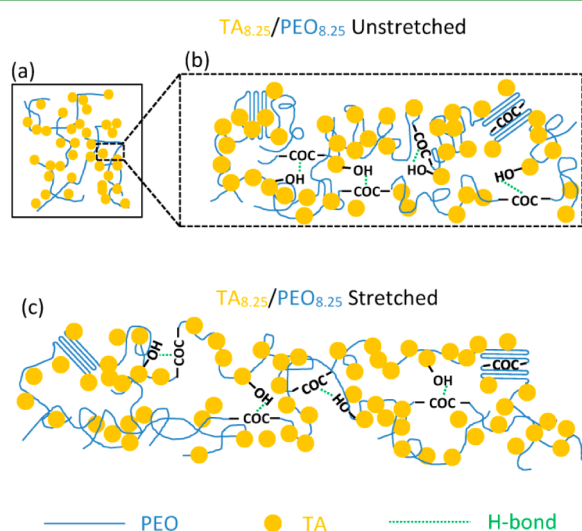


Figure 4. Schematic showing the change in TA/PEO structure (a, b) before and (c) during stretching.

has a much higher bond strength than van der Waals forces between PEO chains, so the deformation is more likely to be a result of PEO chain segment reorientation and extension rather than breaking TA-PEO hydrogen bonds. Future experiments are needed to clarify the change in H-bonding before and after stretching, in order to validate this deformation mechanism. All of this causes the TA/PEO assembly to be highly elastomeric in nature (Figure 4c). Furthermore, a single stretch results in very few bonds being broken, so the TA/PEO assembly is able to retain its gas barrier up to 100% strain. As shown in Figure 2, a modest loss of gas barrier occurs with cyclic strain to 100%, possibly due to gradual breakage of hydrogen bonds.³²

In conclusion, by replacing PAA with TA as the H-bonding donor, fully elastomeric gas barrier thin films can be deposited layer-by-layer. The superior elasticity of the TA/PEO assembly originates from its unique microstructure, which can be tailored by altering deposition pH. At low pH (≤ 7), TA forms a rigid network through self-association that imparts high modulus to the TA/PEO assembly. By increasing the ionization of TA at higher pH (>7), the formation of this rigid network is inhibited due to reduced self-association and lower TA content in the film. TA/PEO thin films assembled at pH 8.25 not only exhibit

a permeability that is 1 order of magnitude lower than pure PEO, but also display better gas barrier retention than fully polymeric assemblies (e.g., PAA/PEO). No loss of gas barrier was observed after a single 100% stretch, which is a remarkable improvement over PAA/PEO, whose OTR increased by 70%. Although repeated extension to 100% strain leads to somewhat reduced gas barrier in the TA/PEO assembly, likely due to breaking of H-bonds, the level of reduction is relatively small. The TA/PEO assembly introduced here is a significant step forward, offering a practical solution for improving the gas barrier of elastomeric pressurized objects, such as tires or blimps.

■ ASSOCIATED CONTENT

Supporting Information

The Supporting Information is available free of charge on the ACS Publications website at DOI: 10.1021/acsami.5b04500.

Experimental information, tannic acid content, and surface morphology (PDF)

■ AUTHOR INFORMATION

Corresponding Author

*E-mail: jgrunlan@tamu.edu. Phone: 979-845-3027.

Present Address

‡F.X. is currently at National Energy Technology Laboratory, 626 Cochran Mill Road, Pittsburgh, PA 15236, USA

Notes

The authors declare no competing financial interest.

■ ACKNOWLEDGMENTS

The authors acknowledge the Texas A&M Engineering Experiment Station (TEES) and the Texas A&M University Materials Characterization Facility (MCF) for infrastructural support of this research.

■ REFERENCES

- (1) Decher, G. Fuzzy Nanoassemblies: Toward Layered Polymeric Multicomposites. *Science* **1997**, *277*, 1232–1237.
- (2) Picart, C.; Lavalle, P.; Hubert, P.; Cuisinier, F. J. G.; Decher, G.; Schaaf, P.; Voegel, J. C. Buildup Mechanism for Poly(L-lysine)/Hyaluronic acid Films onto a Solid Surface. *Langmuir* **2001**, *17*, 7414–7424.
- (3) Schmitt, J.; Gruenewald, T.; Decher, G.; Pershan, P. S.; Kjaer, K.; Loesche, M. Internal Structure of Layer-by-Layer Adsorbed Polyelectrolyte Films: a Neutron and X-ray Reflectivity Study. *Macromolecules* **1993**, *26*, 7058–7063.
- (4) Kharlampieva, E.; Kozlovskaya, V.; Anker, J. F.; Sukhishvili, S. A. Hydrogen-Bonded Polymer Multilayers Probed by Neutron Reflectivity. *Langmuir* **2008**, *24*, 11346–11349.
- (5) Yang, Y.-H.; Bolling, L.; Priolo, M. A.; Grunlan, J. C. Super Gas Barrier and Selectivity of Graphene Oxide-Polymer Multilayer Thin Films. *Adv. Mater.* **2013**, *25*, 503–508.
- (6) Hagen, D. A.; Foster, B.; Stevens, B.; Grunlan, J. C. Shift-Time Polyelectrolyte Multilayer Assembly: Fast Film Growth and High Gas Barrier with Fewer Layers by Adjusting Deposition Time. *ACS Macro Lett.* **2014**, *3*, 663–666.
- (7) Mølgaard, S. L.; Henriksson, M.; Cárdenas, M.; Svagan, A. J. Cellulose-Nanofiber/Polygalacturonic Acid Coatings with High Oxygen Barrier and Targeted Release Properties. *Carbohydr. Polym.* **2014**, *114*, 179–182.
- (8) Pan, H.; Wang, W.; Pan, Y.; Song, L.; Hu, Y.; Liew, K. M. Formation of Self-Extinguishing Flame Retardant Biobased Coating on Cotton Fabrics via Layer-by-Layer Assembly of Chitin Derivatives. *Carbohydr. Polym.* **2015**, *115*, 516–524.

- (9) Apaydin, K.; Laachachi, A.; Fouquet, T.; Jimenez, M.; Bourbigot, S.; Ruch, D. Mechanistic Investigation of a Flame Retardant Coating Made by Layer-by-Layer Assembly. *RSC Adv.* **2014**, *4*, 43326–43334.
- (10) Chang, J.; Huang, X.; Zhou, G.; Cui, S.; Hallac, P. B.; Jiang, J.; Hurley, P. T.; Chen, J. Multilayered Si Nanoparticle/Reduced Graphene Oxide Hybrid as a High-Performance Lithium-Ion Battery Anode. *Adv. Mater.* **2014**, *26*, 758–764.
- (11) Cho, C.; Stevens, B.; Hsu, J.-H.; Bureau, R.; Hagen, D. A.; Regev, O.; Yu, C.; Grunlan, J. C. Completely Organic Multilayer Thin Film with Thermoelectric Power Factor Rivaling Inorganic Tellurides. *Adv. Mater.* **2015**, *27*, 2996–3001.
- (12) Kim, Y.; Zhu, J.; Yeom, B.; Di Prima, M.; Su, X.; Kim, J.-G.; Yoo, S. J.; Uher, C.; Kotov, N. A. Stretchable Nanoparticle Conductors with Self-Organized Conductive Pathways. *Nature* **2013**, *500*, 59–63.
- (13) Sukhishvili, S. A.; Granick, S. Layered, Erasable Polymer Multilayers Formed by Hydrogen-Bonded Sequential Self-Assembly. *Macromolecules* **2002**, *35*, 301–310.
- (14) Broderick, A. H.; Manna, U.; Lynn, D. M. Covalent Layer-by-Layer Assembly of Water-Permeable and Water-Impermeable Polymer Multilayers on Highly Water-Soluble and Water-Sensitive Substrates. *Chem. Mater.* **2012**, *24*, 1786–1795.
- (15) Stevens, B.; Dessiatova, E.; Hagen, D. A.; Todd, A. D.; Bielawski, C. W.; Grunlan, J. C. Low-Temperature Thermal Reduction of Graphene Oxide Nanobrick Walls: Unique Combination of High Gas Barrier and Low Resistivity in Fully Organic Polyelectrolyte Multilayer Thin Films. *ACS Appl. Mater. Interfaces* **2014**, *6*, 9942–9945.
- (16) Zhuk, A.; Mirza, R.; Sukhishvili, S. Multiresponsive Clay-Containing Layer-by-Layer Films. *ACS Nano* **2011**, *5*, 8790–8799.
- (17) Lutkenhaus, J. L.; Hrabak, K. D.; McEnnis, K.; Hammond, P. T. Elastomeric Flexible Free-Standing Hydrogen-Bonded Nanoscale Assemblies. *J. Am. Chem. Soc.* **2005**, *127*, 17228–17234.
- (18) Lutkenhaus, J. L.; McEnnis, K.; Hammond, P. T. Tuning the Glass Transition of and Ion Transport within Hydrogen-Bonded Layer-by-Layer Assemblies. *Macromolecules* **2007**, *40*, 8367–8373.
- (19) Xiang, F.; Ward, S. M.; Givens, T. M.; Grunlan, J. C. Super Stretchy Polymer Multilayer Thin Film with High Gas Barrier. *ACS Macro Lett.* **2014**, *3*, 1055–1058.
- (20) Xiang, F.; Ward, S. M.; Givens, T. M.; Grunlan, J. C. Structural Tailoring of Hydrogen-Bonded Poly(Acrylic Acid)/Poly(Ethylene Oxide) Multilayer Thin Films for Reduced Gas Permeability. *Soft Matter* **2015**, *11*, 1001–1007.
- (21) Erel-Unal, I.; Sukhishvili, S. A. Hydrogen-Bonded Multilayers of a Neutral Polymer and a Polyphenol. *Macromolecules* **2008**, *41*, 3962–3970.
- (22) Liu, F.; Kozlovskaya, V.; Zavgorodnya, O.; Martinez-Lopez, C.; Catledge, S.; Kharlampieva, E. Encapsulation of Anticancer Drug by Hydrogen-Bonded Multilayers of Tannic Acid. *Soft Matter* **2014**, *10*, 9237–9247.
- (23) Chen, J.; Kozlovskaya, V.; Goins, A.; Campos-Gomez, J.; Saeed, M.; Kharlampieva, E. Biocompatible Shaped Particles from Dried Multilayer Polymer Capsules. *Biomacromolecules* **2013**, *14*, 3830–3841.
- (24) Lybaert, L.; De Vlieghere, E.; De Rycke, R.; Vanparijs, N.; De Wever, O.; De Koker, S.; De Geest, B. G. Bio-Hybrid Tumor Cell-Templated Capsules: A Generic Formulation Strategy for Tumor Associated Antigens in View of Immune Therapy. *Adv. Funct. Mater.* **2014**, *24*, 7139–7150.
- (25) Dierendonck, M.; Fierens, K.; De Rycke, R.; Lybaert, L.; Maji, S.; Zhang, Z.; Zhang, Q.; Hoogenboom, R.; Lambrecht, B. N.; Grooten, J.; Remon, J. P.; De Koker, S.; De Geest, B. G. Nanoporous Hydrogen Bonded Polymeric Microparticles: Facile and Economic Production of Cross Presentation Promoting Vaccine Carriers. *Adv. Funct. Mater.* **2014**, *24*, 4634–4644.
- (26) Ejima, H.; Richardson, J. J.; Liang, K.; Best, J. P.; van Koeverden, M. P.; Such, G. K.; Cui, J.; Caruso, F. One-Step Assembly of Coordination Complexes for Versatile Film and Particle Engineering. *Science* **2013**, *341*, 154–157.
- (27) Holder, K. M.; Spears, B. R.; Huff, M. E.; Priolo, M. A.; Harth, E.; Grunlan, J. C. Stretchable Gas Barrier Achieved with Partially Hydrogen-Bonded Multilayer Nanocoating. *Macromol. Rapid Commun.* **2014**, *35*, 960–964.
- (28) Charlton, A. J.; Baxter, N. J.; Khan, M. L.; Moir, A. J. G.; Haslam, E.; Davies, A. P.; Williamson, M. P. Polyphenol/Peptide Binding and Precipitation. *J. Agric. Food Chem.* **2002**, *50*, 1593–1601.
- (29) Coleman, M. M.; Skrovanek, D. J.; Hu, J.; Painter, P. C. Hydrogen Bonding in Polymer Blends. 1. FTIR Studies of Urethane-Ether Blends. *Macromolecules* **1988**, *21*, 59–65.
- (30) Ratna, D.; Divekar, S.; Samui, A. B.; Chakraborty, B. C.; Banthia, A. K. Poly(Ethylene Oxide)/Clay Nanocomposite: Thermomechanical Properties and Morphology. *Polymer* **2006**, *47*, 4068–4074.
- (31) Wang, H.; Keum, J. K.; Hiltner, A.; Baer, E.; Freeman, B.; Rozanski, A.; Galeski, A. Confined Crystallization of Polyethylene Oxide in Nanolayer Assemblies. *Science* **2009**, *323*, 757–760.
- (32) Wang, C.; Wu, H.; Chen, Z.; McDowell, M. T.; Cui, Y.; Bao, Z. Self-Healing Chemistry Enables the Stable Operation of Silicon Microparticle Anodes for High-Energy Lithium-Ion Batteries. *Nat. Chem.* **2013**, *5*, 1042–1048.